A novel fuel injected mass feedback-control for single and multiple injections in direct injection systems for CI engines

A novel fuel injected mass feedback-control for single and multiple injections in direct injection systems for CI engines

Ferrari A.[(*,a)], Novara C.[(b)], Vento O.[(a)], Violante M.[(c)], Zhang T.[(d)]

[a] *Energy Department, Politecnico di Torino, Turin, Italy*
[b] *Electronics and Telecommunications Department,, Politecnico di Torino, Turin, Italy*
[c] *Control and Computer Engineering Department, Politecnico di Torino, Turin, Italy*
[d] *College of Mechanical and Vehicle Engineering, Hunan University, Changsha, China*

(*) Corresponding author. Email: alessandro.ferrari@polito.it Phone +390110904426

Abstract

A new feedback-control capable to enhance the fuel injected quantity accuracy has been proposed and tested. The experimental pressure in the rail and that measured along the rail-to-injector pipe, in the vicinity of the injector inlet, have been used as input data to a home-made hydraulic model. By means of this model the pressure downstream of the gauged orifice at the interface between the rail and the rail-to-injector pipe is determined; the mass at the injector inlet can be obtained by means of an integration of the estimated flow-rate entering the injector. A robust mathematical law can be established between the mass that enters the injector and the one injected, thus, a feedback-control based on the error between the target injected quantity stored in the ECU and the predicted injected mass has been designed and implemented for the *ET* correction. The new feedback-strategy has been applied to control both single and double (pilot-main) schedules by using a rapid prototyping hardware. Regarding single shots, the new control results to be capable of reducing the injected mass inaccuracy, which is due to the different thermal regimes experienced by the injector, below 0.6 mg (the standard open loop control can feature an error up to 2 mg when the fuel tank temperature is varied), while for the pilot-main schedules it is possible to dramatically reduce the inaccuracy on the desired overall injected quantity (below 1 mg) when digital or continuous rate shaping programs are implemented.

Keywords

Injected mass control; fuel injection system; compression ignition engine, rapid prototyping hardware; renewable diesel oil.

Highlights

- A novel feedback-control strategy for the injected quantity is built up.
- A rapid prototyping hardware is used to test the developed control.
- Single and multiple injection performance of the prototypal hardware is analyzed.

Introduction

In the last years, environmental protection agencies have concentrated on internal combustion engine (ICE) emissions, due to their effect on environment and health [1]. For this reason, researchers have been focused on this topic, looking for solutions that are capable to reduce the ICE impact on environment and living beings [2, 3].

Nowadays, diesel engines are still playing a key-role as a power source [4] and numerous studies have been developed regarding this category of engines, in which almost all the aspects are taken into account. The shape of the combustion chamber, influencing the fuel-air mixing, can affect the soot formation and, therefore, the smoke emissions [5]. It has been demonstrated that the consistency of the engine assembly influences the NO_x emissions, for example due to a varied combustion temperature leaded by the different nozzle extension height [6]. A valid approach in the reduction of pollutant emissions should also consider the refinement of the after-treatment devices such as the diesel oxidation catalyst, the diesel particulate filter, lean NO_x trap, and selective catalytic reduction [7].

The Common Rail (*CR*) fuel injection system has added available parameters to reach an optimum engine calibration for the widest range of working conditions, thanks to its increasing value of maximum injection pressure, that can go beyond 3000 bar [8], the elevated number of injection events

for combustion cycle and the flexibility in injection timings [9]. The split ratio of a triple injection strategy has been analysed to determine its effect on the ignition delay, unburned emissions, and combustion noise (CN) [10]. For a HCCI engine operating with a multiple fuel shot strategy, if the first injection pulse duration is increased, the diffusion phase combustion will be minimized, reducing the heat release rate, thereby diminishing NO_x and soot [11].

Concerning to injected flow-rate pattern, it has been shown that for low and medium loads, the optimum engine calibration should feature triple or quadruple injections together with possible rate shaping schedules, leading to an enhancement in the soot-NO_x trade-off and a reduction in the CN [12]. In particular, the digital-rate shaping strategy (the two injections are very close, but can still be distinguished from one another) can improve the overall engine brake specific fuel consumption and a consequent reduction in the CO_2 emissions is achieved [13]. These complex injection strategies can be implemented with either a solenoid or piezoelectric injectors [17].

However, if the dwell time (DT) is dramatically reduced to adopt strategies such as the aforementioned digital-rate shaping or the continuous rate shaping (the two injection events are merged together), significant cyclic variation in the engine torque occurs, due to injector-to-injector and cyclic differences regarding the rates of injections, thus representing a potential issue for the engine implementation [14]. In fact, when the electric DT goes below a particular value, the overall fuel injected quantity generally features anomalous increasing, hence a small change in the hydraulic dwell time can lead to an important influence on the fuel injected mass [15, 16].

This context justifies the efforts on the development of robust feedback-control strategies for the fuel injected quantity, which is usually treated by means of an open-loop approach. Indeed, in standards common rail system, the injected mass is predicted, based on the duration of the electrical current signal (ET) and the nominal rail pressure (p_{nom}) [18]: these two values are stored onto the ECU calibration maps, defined by means of preliminary experimental campaigns and there is no feedback control on the effective injected mass [19].

77 An estimation technique of the fuel injected mass has been obtained by measuring the in-cylinder
78 pressure signal [20]. An already validated predictive combustion model has been applied contrariwise.
79 The overall heat transferred by the charge to the walls over the combustion period is estimated and,
80 with the acquired in-cylinder pressure, the released net energy is derived. Finally, an estimation of the
81 injected fuel mass is obtained by calculating the chemical energy of the injected fuel.

82 The feedback strategy proposed in [21] predicts the pilot mass estimation by means of the pilot
83 misfire ratio. Misfire occurs when the pilot injected quantity is not able to burn and, consequently, an
84 increased premixed peak of the main injection combustion takes place. Since the misfire probability is
85 well correlated with the pilot mass [22], the pilot injected mass can be predicted, after a preliminary
86 characterization of the misfire events, using an in-cylinder pressure transducer applied to detect the
87 misfire. In [21], the correlation between the pilot injected mass and the pilot misfire ratio is used
88 together with a Bayesian approach.

89 Two robust feedback-control strategies have been developed for both single and pilot-main shots, by
90 means of the measurement of the flow-rate entering the injector [23, 24]. It has been shown that the
91 mass entering the injector, obtained through an integration of the measured flow-rate, correlates well
92 with the effective injected quantity. Hence, a feedback-control to modify the energizing time (*ET*) to
93 the injector pilot stage has been established, and the current signal is modified based on the error
94 between the predicted injected mass and the target one.

95 Another technique to estimate the mass entering the injector is based on an artificial neural network
96 [25]. In this case, the input signal is represented by the pressure time distribution measured in the
97 vicinity of the injector inlet.

98 A prediction of the injection temporal length (*ITL*) has been obtained by means of an approach
99 involving the time-frequency analysis [26]. The short-time Fourier transform is applied to the pressure
100 trace measured in the proximity of injector inlet, then the mean instantaneous frequency (*MIF*) trace
101 is determined and is used to develop a needle-lift virtual sensor. The injected mass can be estimated

by means of the *ITL* prediction, that is given by the distance between two local maximums of the *MIF* trace.

Compensative strategies for the injected mass have been introduced by injection systems manufacturers, which have produced superior injectors featuring additional devices to mitigate the inaccuracy of the fuel injected quantity. Bosch developed an injector equipped with a force transducer (labelled as Needle Closing Sensors), that acquires the pressure force induced by the fuel inside the control chamber. Some noteworthy instants regarding the needle motion can be recognized by means of this force time history and they are used as input data to an algorithm which estimates the injected fuel quantity [27]. The i-Art technology designed by DENSO is able to measure the pressure in the control chamber by means of a piezoelectric pressure sensor installed to the injector pilot stage. This pressure signal is used to predict the injected mass with a complex transfer function [28, 29]. Finally, Delphy has proposed the "Switch" technology. The non-ballistic needle is inserted inside an electric circuit where the voltage is detected. When the needle closes the nozzle, or it reaches its upper stroke end the circuit closes in two distinct manners. Therefore, if the voltage is detected, the two corresponding time instants can be identified, and the injected quantity can be estimated by means of a needle lift-based submodel [30].

In this work, an innovative feedback-control strategy to reduce the inaccuracy of the fuel injected quantity is presented and tested. The proposed algorithm receives as input datum the measurement of the pressure traces inside the rail and along the pipe that feeds the injector, in the vicinity of the injector inlet. The mass which enters the injector can be estimated based on these pressure signals and, by means of a correlation, the predicted injected mass is obtained. The new feedback-control has been implemented in a rapid prototyping hardware. Different fuel tank temperatures have been taken into account to analyse single injections, while for pilot-main shots the total injected mass has been measured in the short *DT* range. The new strategy represents an evolution of that developed in [23, 24] because the installation of only one additional pressure transducer is required in the commercial *CR* injection system layout.

Experimental facility

The hydraulic tests have been performed at the Politecnico di Torino ICE Laboratory, at a Moehwald-Bosch hydraulic test bench (nominal power: 35 kW, maximum speed: 6100 rpm, maximum torque: 100 Nm). Different thermocouples and piezoresistive pressure transducers are used to monitor the temperature and the pressure levels in various locations of the analysed high-pressure hydraulic circuit. A HDA flowmeter [31] measures the injected flow-rate traces that are integrated to obtain the corresponding masses, while injector fuel leakages are evaluated by means of a KMM flowmeter.

The adopted calibration fluid at the test rig is a Shell V-Oil 1404 (ISO 4113), since it is capable to satisfactorily reproduce the renewable diesel oil properties over a proper range of pressure and temperature values (at least up to 120°C).

The selected injection system for the experimental campaign is a last generation Bosch CR system. The rail (with a capacitance of 10 cm^3) is fed by a high-pressure pump featuring a displacement of 430 mm^3 with a double effect single piston and a transmission ratio with the engine equals to 1:1. Four CRI 2.20 (solenoid-actuated) injectors are connected to the rail by means of high-pressure pipes with a length of 320 mm and an internal diameter of 2.8 mm."

The injector pilot stages feature a pressure-balanced pilot-valve. Moreover, they present an integrated Minirail. Figure 1 presents the scheme of the tested injector.

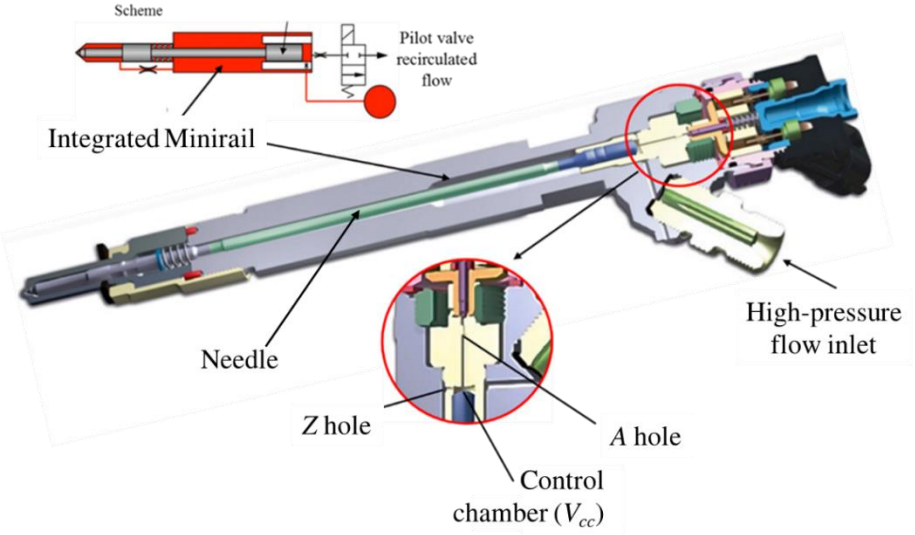

Figure 1. Injector CRI 2.20.

Concerning the injector working principle, a part of fuel entering the injector from the injector-feeding pipe fills, through the Z hole, the control chamber (volume V_{cc}), and the other part reaches the integrated Minirail. The injection starts after the electronic control unit (ECU) has switched on the electrical current I to the pilot valve solenoid. Consequently, the control chamber is discharged through the A hole and the needle moves up opening the nozzle. The control chamber pressure starts again to rise at the end of the current signal provided by the *ECU*, and the needle closure phase is induced. The hydraulic end of the injection is achieved when the needle closes the nozzle reaching its downstroke end [32].

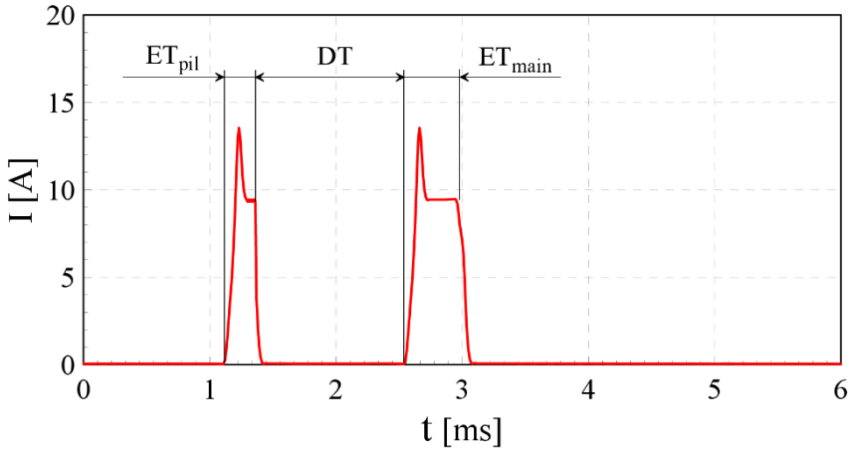

Figure 2. Example of a pilot-main injection current signal.

Both single and pilot-main injections have been taken into account and the considered nominal rail pressure levels (p_{nom}) varied in the range 500-1800 bar. Tests on single injections have been performed by considering different *ET* values. Regarding the pilot-main injections, different combination of ET_{pil}, ET_{main} and *DT* have been selected, and their meaning is shown in Fig. 2. Pertaining to pilot-main injections, different rail pressure levels have been selected and, for each of them, the same main and pilot injected quantities have been chosen: 15 mg, 20 mg or 30 mg for the main injection and 1.5 mg or 3 mg for the pilot injection. The dwell time has been varied from 100 µs to 500 µs.

The selected pump speed for the entire experimental campaign was 2000 rpm, corresponding to 2000 rpm of engine speed.

Algorithm of the feedback-control and rapid prototyping hardware

Figure 3 shows the injection system layout. A pressure sensor mounted at one rail extremity is used to monitor the rail pressure time history $p_{rail}(t)$. The nominal rail pressure control strategy and the one pertaining to the modulation of the *ET* to the injector have been developed on Matlab Simulink.

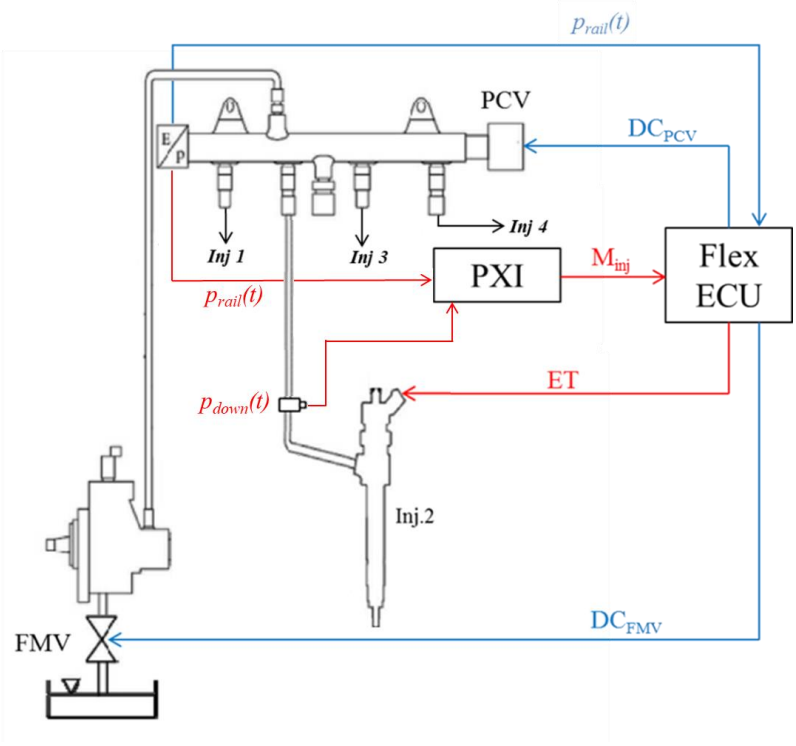

Figure 3. The layout of the tested injection system (blue refers to p_{rail} control system and red to M_{inj} control system).

Opposite the rail pressure sensor, the pressure control valve (*PCV*) is installed (cf. Fig 3). This valve is employed to control and maintain the nominal rail pressure p_{nom} target (provided by the *ECU*). A closed-loop control is set up by monitoring $p_{rail}(t)$, throttling the excess of the pumped fuel. The rail pressure can also be controlled through the fuel-metering valve (*FMV*) that is installed at the pump inlet. By acting on the *FMV*, the flow-rate entering the pump is modified based on the injector requirements and the flow-rate throttled by the *PCV* is ideally null [33].

A scheme of the implemented injection system control strategies is reported in Fig. 4. The rail pressure signal is acquired with a frequency of 200 Hz by the ECU, giving the filtered signal $p_{filter}(t)$ (block H2). The difference $e(t)$ between p_{nom} and $p_{filter}(t)$ is computed and is received as an input by block R2, where the *PID* controller for the rail pressure is usually implemented in commercial

systems. This controller generates the duty cycle value to be provided to the valve selected for the pressure control (*FMV* or *PCV*).

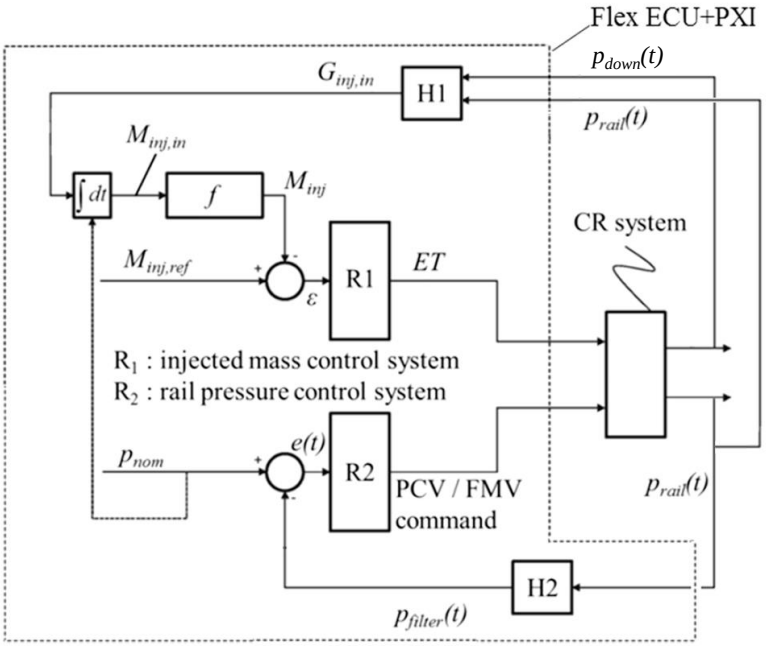

Figure 4. The injection system control strategies.

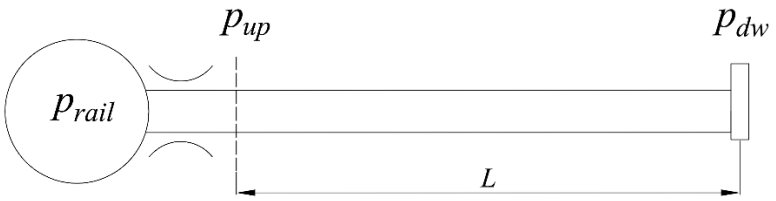

Figure 5. Scheme of the hydraulic model.

The new control strategy shown in Fig. 4 consists in the injected mass feedback-control and the installed hardware has been simplified compared to that installed in [23, 24]. The measured pressure signals $p_{down}(t)$ (acquired near the injector inlet, cf. Fig. 3) and $p_{rail}(t)$ are sufficient to determine the mass flow-rate time history entering the injector. Unlike the prototype in [23, 24], as is shown in Fig. 3, it is therefore enough to install only one pressure sensor along the injector-feeding pipe.

In block H1 (cf. Fig. 4), which receives $p_{rail}(t)$ and $p_{down}(t)$ as input (acquired with a frequency of 30 kHz, that is much higher than the standard sampling frequency used in the H2 block for the rail pressure control), a simple hydraulic model is implemented. In this model, represented in Fig. 5, the rail is assumed as a zero-dimensional chamber at which the measured pressure $p_{rail}(t)$ is imposed as a

boundary condition. The rail is connected to the injector-feeding pipe by means of a gauged orifice (its used in the commercial layout as a passive damper for the free pressure waves triggered by the nozzle closure [34]), characterized by a restricted area A_{res} (obtained by measuring the gauged orifice diameter, equals to d_{res}=1 mm) and a flow coefficient C_d=0.8 (this value has been fitted on flow-rates values at the injector inlet obtained by applying other techniques presented in [23, 24]). Close to the downstream extremity of the high-pressure pipe with cross-section area *A*, the measured pressure time history $p_{down}(t)$ is assigned as the second boundary condition at a distance *L* from the orifice outlet. The pressure $p_{up}(t)$ represents the pressure trace measured at the inlet of the injector-feeding pipe (cf. Fig 5) and is an unknown quantity. The instantaneous flow-rate G_{or} flowing through the gauged orifice can be expressed as:

$$\begin{cases} G_{or} = -\mathrm{C_d} \cdot \mathrm{A_{res}} \cdot \sqrt{2 \cdot (\mathrm{p_{up}} - \mathrm{p_{rail}})\rho} & \text{if} \quad p_{up} > p_{rail} \\ G_{or} = \mathrm{C_d} \cdot \mathrm{A_{res}} \cdot \sqrt{2 \cdot (\mathrm{p_{rail}} - \mathrm{p_{up}})\rho} & \text{if} \quad p_{rail} > p_{up} \end{cases} \tag{1}$$

where ρ represents the flow density.

The continuity equation and the momentum balance equation for the piece of pipe with length *L* have been combined. By neglecting the wall shear stress and with the assumption of 1D incompressible flow, one obtains

$$\frac{\partial u}{\partial t} + \frac{1}{\rho}\frac{\partial p}{\partial x} = 0 \tag{2}$$

where *u* and *p* stand for the 1D velocity and pressure, respectively, and *x* represents the spatial coordinate along the pipe axis.

Multiplying Eq. (2) by ρA (ρ is the flow density), integrating over the distance *L* and dividing by the same distance *L*, on has:

$$\frac{\mathrm{d}\bar{G}}{\mathrm{d}t} = \frac{A}{L}\,(\mathrm{p_{up}} - \mathrm{p}_{down}) \tag{3}$$

where $\bar{G}$ represents the space-averaged instantaneous flow-rate. By integrating Eq. (3) with respect to the time, one obtains:

$$\bar{G} = \int_0^t \frac{A}{L} \cdot (\mathrm{p_{up}} - \mathrm{p}_{down})\, dt \tag{4}$$

It can be assumed that $G_{or} \approx \bar{G}$ [35]. Eqs. (1) and (4) can therefore be solved together and the two unknown variables, namely the pressure p_{up} and the flow-rate G_{or} traces, can be evaluated.

The flow-rate that reaches the injector is evaluated by means of [23, 24]:

$$G_{inj,in} = \frac{A}{L}\int_0^t \Delta p dt - \frac{A}{L}\langle \Delta p \rangle \cdot t \tag{5}$$

where $\Delta p = p_{up} - p_{down}$ and $\langle \Delta p \rangle$ stands for the Δp time-averaged value for the considered injection cycle. This flow-rate represents the output of block H1 (cf. Fig. 4) and by integrating it over time instants t_i and t_f, the injector inlet mass $M_{inj,in}$ is obtained:

$$M_{inj,in} = \int_{t_i}^{t_f} G_{inj,in} dt \tag{6}$$

In Fig. 6, two different flow-rates for single and double injection are represented. The integration performed in Eq. 6 to obtain $M_{inj,in}$ starts in correspondence of the time instant at which the electrical current begins to rise (in Fig. 6 one has $t_i = 0$), and it stops at the time instant where the $G_{inj,in}(t)$ trace features its absolute maximum [23, 24]. The negative flow-rates that can be inferred in Fig. 6 are due to the pressure waves travelling back and forth along the pipe that feeds the injector, which are caused by the nozzle closure. These physical contributions are not taken into account since they occur after t_f.

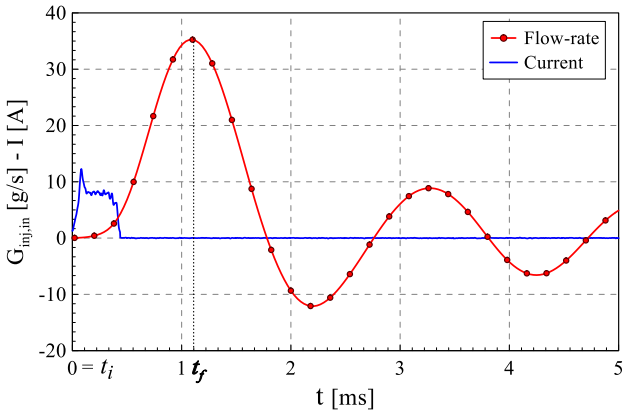

(a): Single injection (p_{nom} = 1200 bar, $M_{inj,ref}$ = 20 mg).

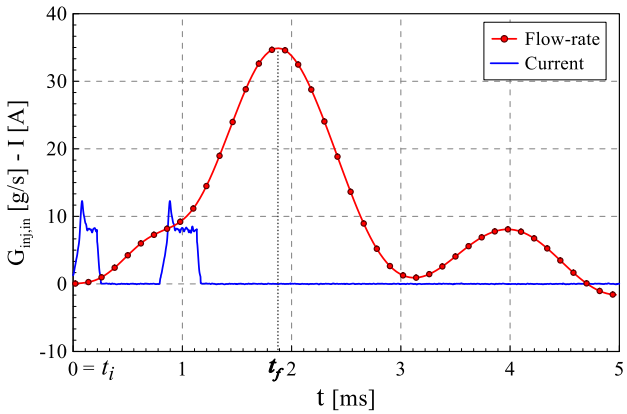

(b): Pilot-main injection (p_{nom} = 1600 bar, $M_{inj,pil}$ = 3 mg, , $M_{inj,main}$ = 30 mg, DT = 500 µs)

Figure 6. Flow-rates time histories entering the injector for a single (a) and a pilot-main (b) injection.

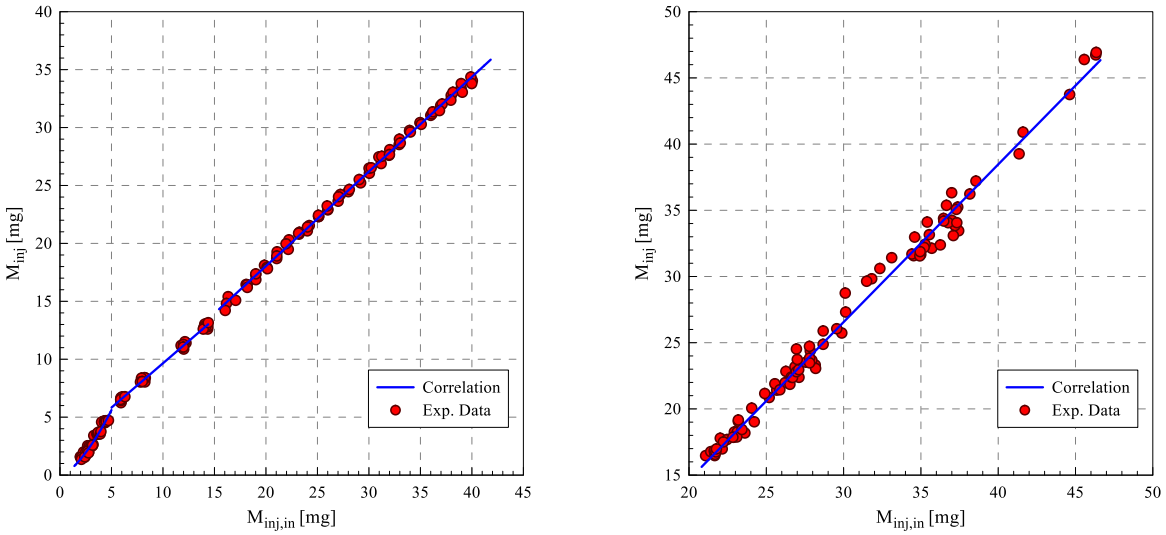

(a): Single injections. *(b): Pilot-main injections*

Figure 7. Mathematical laws to determine the injected fuel quantity from the injector inlet one.

Figure 7 shows that the fuel injected quantity (M_{inj}) correlates well with the fuel amount that enters the injector ($M_{inj,in}$). This is verified for both single (cf. Fig. 7a) and pilot-main injections (cf. Fig. 7b, where the M_{inj} data refer to the overall injected quantities during the different injection events). Mathematical laws, namely $M_{inj}=f(M_{inj,in})$, reported in Fig. 7 have been obtained by means of a fitting of the experimental points (126 for single injections and 90 for pilot-main schedules, both referring to different rail pressure levels and injected masses). Thanks to these correlations the measurement of $M_{inj,in}$ allows the estimation of M_{inj} during the real system operation. Furthermore, the presented correlations result to be independent with respect to the fuel tank temperature (T_{tank}) [23, 24]. Quantity ε is calculated by subtracting the prediction of the injected amount M_{inj} to the desired target value ($M_{inj,ref}$), stored in the ECU, This difference reaches, as an input, block R1 (cf. Fig. 4), which contains

a *PID* controller that calculates the corrected *ET* that can mitigate the inaccuracy of the fuel injected quantity for the next injection event. In Fig. 3, the hardware components employed for the new control strategy are represented. A National Instrument PXI platform has been used to receive the signals from the sensors of p_{rail} and p_{down} and to implement Eqs. (1), (4)-(6) and the mathematical laws given by $M_{inj}=f(M_{inj,in})$. A CAN interface cable is used to deliver the injected mass prediction from the PXI platform to the ETAS Flexible ECU, which generates the energizing time to the injectors.

A *ECU* software is usually split into two parts: the first, generally provided by the injection system manufacturer, is the basic software, which contains all the basic information (e.g., the instructions to connect the different pins with the injection system actuators) and the second, called application software, contains the control strategies, such as the pressure and the *ET* ones. ETAS EHOOKS software is used to merge the two aforementioned software and to provide a single software that is finally flashed in the Flexible ECU.

Results and discussion

For a selected working condition, in terms of different values of nominal pressure and target injected mass, the HDA flowmeter has measured the effectively injected fuel quantity (M_{inj}) averaged over 100 consecutive engine cycles. Two different fuel tank temperatures have been selected: 40°C, which is usually selected as reference value from the injection system suppliers, and 68°C, that represents the maximum temperature available in the test bench, for safety reasons.

To assess the injected mass accuracy of the fuel injection system, one can introduce the accuracy $|\Delta M_{inj}|$, given by the absolute value of the difference between the effective-injected mass and the target value. This accuracy is represented along the vertical axis of the 3D diagrams in Figs. 8a, 8b and 8c with respect to both p_{nom} and $M_{inj,ref}$ for single injections. In particular, Figs. 8a, 8b and 8c all refer to the fuel tank temperature T_{tank}= 40°C and they plot data for the standard system with the standard open-loop technique used to control the

injected mass (cf. Fig. 8a), for the previously developed [23] system featuring the closed-loop strategy in which two pressure sensors are involved (cf. Fig. 8b), and for the new system, where the closed-loop control requires only one pressure signal measured along the injector-feeding pipe (cf. Fig. 8c). For all the systems, the pressure is *FMV* controlled based on the difference between p_{nom} and p_{filt}. In Fig. 8, the system with one pressure sensor features similar performance as that of the layout with two additional pressure sensors and its accuracy, which is generally lower than 0.6 mg, slightly improves that of the standard apparatus.

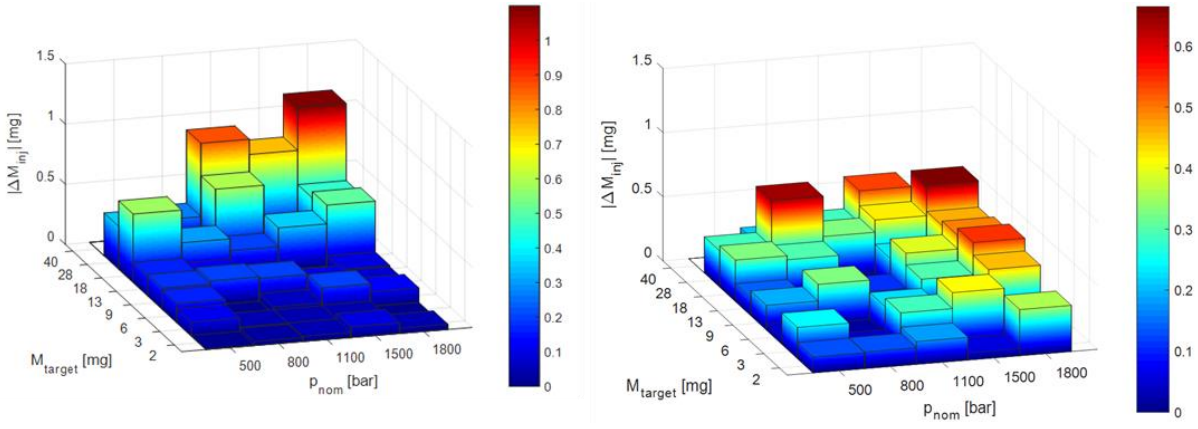

(a): Standard control strategy. *(b): Control strategy with two pressure sensors.*

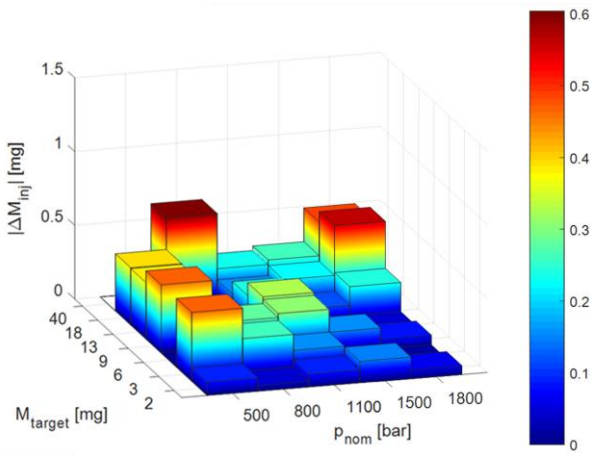

(c): Control strategy with one pressure sensor.

Figure 8. Control strategies performance at T_{tank} = 40°C.

The advantages of the feedback-control strategy for the injected quantity become obvious as T_{tank} increases, as reported in Fig. 9, where T_{tank}=68 °C. In this case, the standard injection

297 system (open-loop control for the injected mass) features an inaccuracy of the injected mass
298 of around 1.5-2.2 mg for significant target mass and high p_{nom} level, as shown in Fig. 9a,
299 while when the new closed-loop control acts the error is below 0.9 mg within the entire range
300 of working condition (cf. Fig. 9c). Furthermore, the performance is in line with that in Fig.
301 9b, where the results of the two additional pressure sensors technique are represented. The
302 fuel temperature affects the injector internal dynamic and modifies the injected quantity for a
303 certain set of *ET* and p_{nom}, since the *ET*-based injector characteristic is temperature dependent
304 [26]. This is evident from the comparison of Figs. 8a and 9a: the standard injection system
305 has the best performance when the T_{tank} value is set to the one at which the standard open-
306 loop control strategy has been tuned, while the accuracy worsens when the fuel temperature
307 augments.
308 Referring to the new control strategy (cf. Figs. 8c and 9c), the inaccuracy is mainly related to
309 the error in the injected mass prediction given by the $M_{inj,in}$-M_{inj} correlation (cf. Fig. 7a,
310 where all the experimental data are inside a bad of ±1 mg of error), while the augment of
311 injected mass lead by the increased fuel temperature can be efficiently contrasted.
312 The normalized standard deviation pertaining to the fuel injected quantity is plotted in the
313 vertical axis of the 3D diagram in Fig. 10 (σ is normalized with respect to the average value
314 of the injected mass and is expressed as a percentage) is reported for the three different
315 control strategies. The standard deviation has been evaluated by means of the HDA over 100

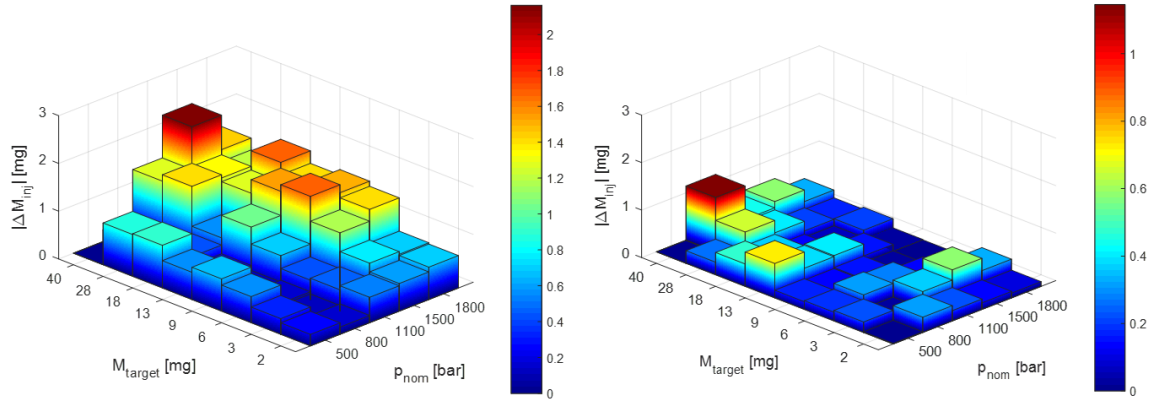

(a): Standard control strategy. *(b): Control strategy with two pressure sensors.*

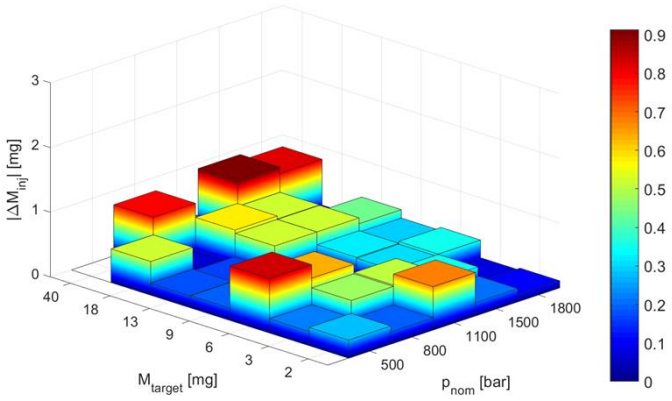

(c): Control strategy with one pressure sensor.

Figure 9. Control strategies performance at T_{tank} = 68°C.

consecutive injections, for different single injection schedules (in terms of *ET*, p_{nom} and T_{tank}). The severe manufacturing tolerances adopted for the CRI 2.20 injector and its Minirail are capable to keep the injection stable, reaching a very satisfactory precision. Regarding the new feedback-control, the precision slightly worsens with respect to the

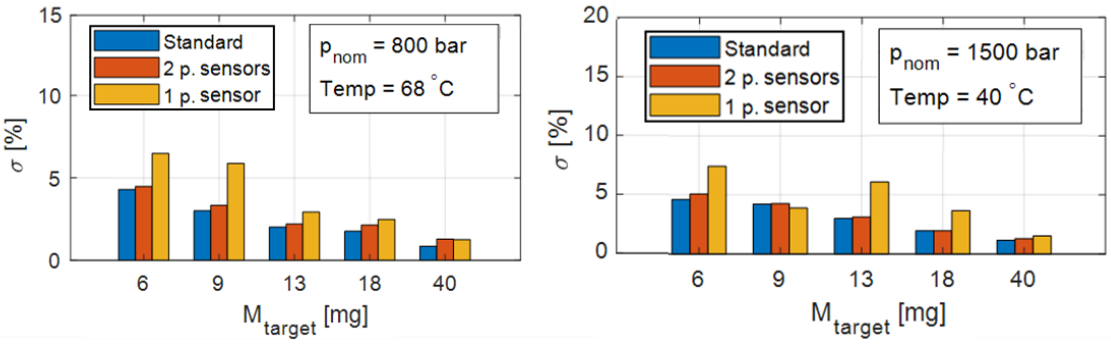

Figure 10. Injected mass normalized standard deviation for different p_{nom} and T_{tank} conditions.

control presented in [23]. However, it must be considered that the purpose of the proposed strategy is aimed at improving the accuracy of the injection system, which can deteriorate, due to physical drifts (such as the thermal one), rather than at enhancing the precision, which affects the small injected masses to a great extent.

Concerning the pilot-main injection, dwell time sweeps have been performed. Figure 11 reports the pattern of the overall injected mass as *DT* varies for different M_{pil}, M_{main} (the pilot and the main injected masses, respectively) and p_{nom} conditions when the injector is controlled by means of the standard open-loop strategy (continuous curves with circle symbols) and the new control-strategy (continuous curves with triangle symbols), compared with the target value (dash dot lines), which is given by the sum of the pilot and main nominal masses. The overall injected mass value is given by summing average values of M_{pil} and M_{main} over 100 consecutive cycles measured by the HDA flowmeter. As can be observed, the standard injection system cannot achieve satisfactory accuracy below DT=300 μs, hence the possibility of applying efficient digital or continuous rate shaping is strongly limited [24]. On the contrary, the new injection system features lower accuracy than 1 mg over the entire 100 μs ÷ 400 μs *DT* range.

Finally, Fig. 12 shows a dynamic test regarding a pilot-main injection whit a target pilot mass (M_{pil}) equals to 2 mg, a target pilot mass (M_{main}) equals to 20 mg, a dwell time of 100 μs, at a nominal pressure of 1000 bar and T_{tank}= 40 °C. Fig. 12a reports the overall injected mass measured for 150 consecutive injections by the HDA (continuous line), compared with the target value (dash-dot line). In the left part of the graph, where the standard open-loop strategy is acting, the error on the total injected mass is around 15 mg (an injection fusion event is considered). When the new control-strategy is switched on (around injection no. 50), after a quick transient, the instantaneous injected mass approaches the target value, leading to a dramatic reduction in the error. Figs. 12b and 12c show two different instantaneous injected

352 flow-rate traces pertaining to the standard control strategy (injection no. 25) and to the new
353 closed-loop control strategy (injection no. 102), respectively.

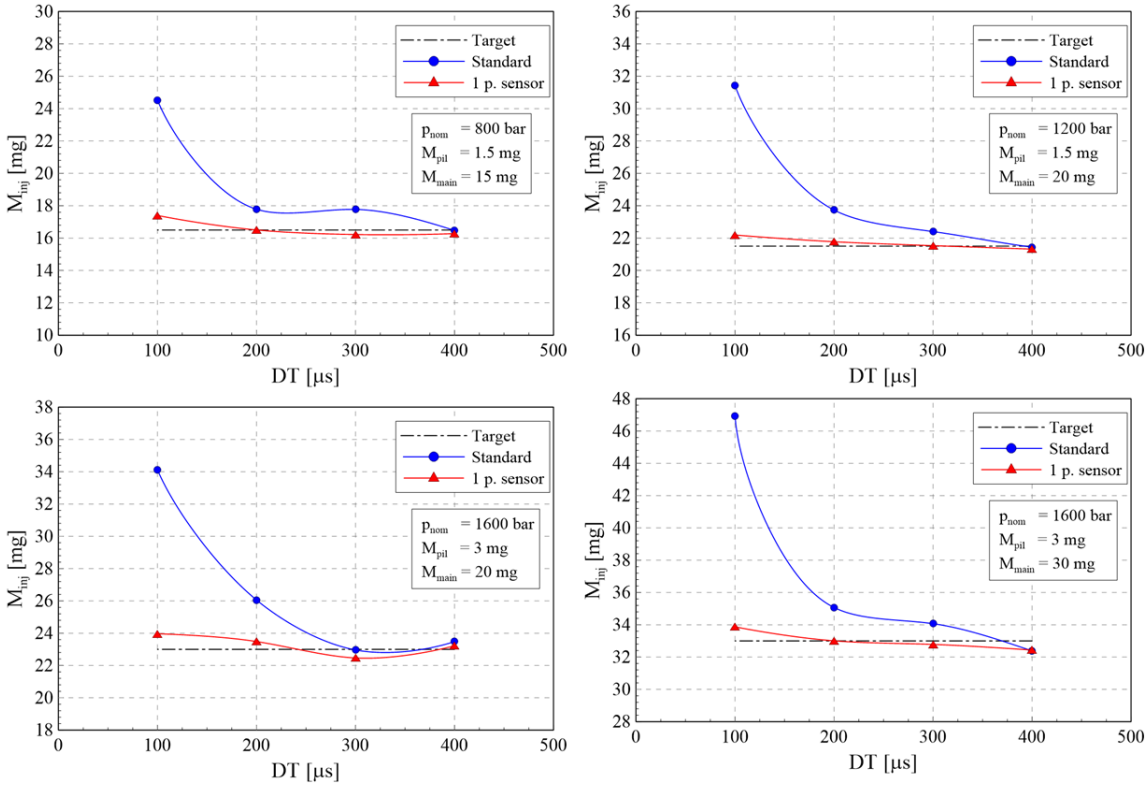

354

355 *Figure 11. Performance of the new control strategy for pilot-main injections.*

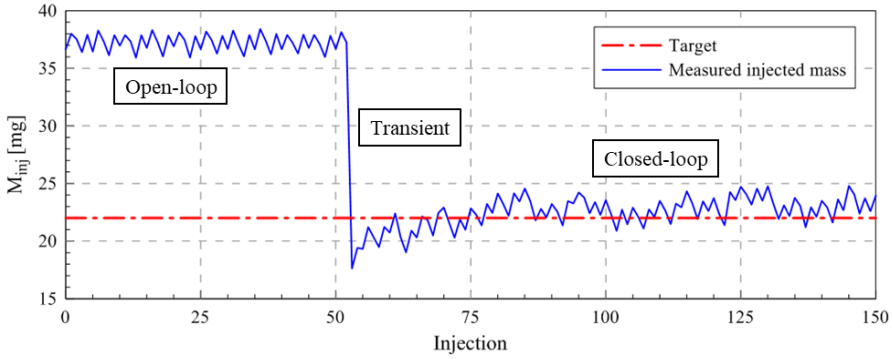

356

357 *(a): Overall injected mass for 150 consecutive injections.*

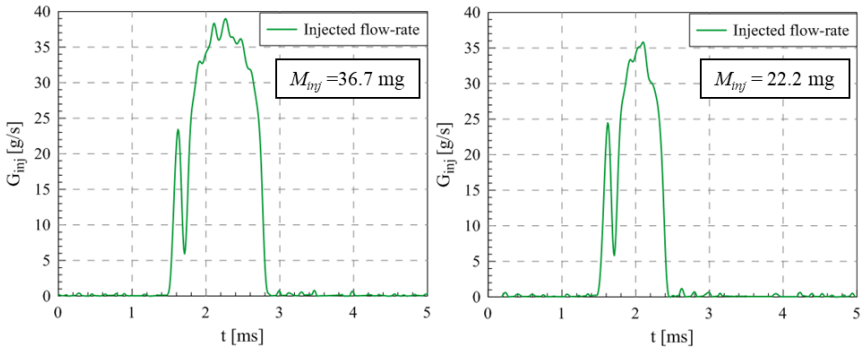

(b): Injected flow-rate time history (standard control). *(c): Injected flow-rate time history (closed-loop control).*

Figure 12. Feedback-control activation effect on the injected flow-rate ($M_{inj,pil}$= 2 mg, $M_{inj,main}$= 20 mg, DT= 100 μs, p_{nom}= 1000 bar, T_{tank}= 40 °C)

Conclusion

A new algorithm has been developed to calculate the flow-rate that enters the injector, based on two measured pressure traces: the one inside the rail (on which the rail pressure level in the commercial CR system is based) and the one detected along the injector-feeding pipe, in the proximity of the injector inlet. The developed algorithm for the flow-rate calculation is based on a simple hydraulic model. The rail is modelled as a zero-dimensional chamber, in which the corresponding measured p_{rail} time history is imposed, and this chamber is connected to the injector-feeding pipe by means of a gauged orifice, with specified area and discharge coefficient. The other measured pressure signal is p_{down}, imposed as the second boundary condition. The momentum balance and the continuity equations are solved in conjunction with a steady-state relation and this set of equations gives as outcomes the flow-rate across the orifice and the pressure time history at the orifice exit, namely p_{up}. This pressure signal is used, together with p_{down} to determine the flow-rate trace entering the injector, i.e. $G_{inj,in}$. By integrating $G_{inj,in}$ with respect to time, the mass at the injector inlet is obtained. This mass correlates well with the effective fuel injected quantity, hence two mathematical laws $M_{inj}=f(M_{inj,in})$ (one for single injections and one for pilot-main shots) have been determined. Owing to this correlation, by measuring the mass that enters the injector, one can obtain an estimated value of the real injected mass. A PID controller receives, as

input datum, the error $\Delta M_{inj}=M_{inj}-M_{inj,ref}$, and, based on it, a corrected value of the energizing time acting on the injector is determined, to mitigate the injected quantity inaccuracy.

The presented control strategy has been tested by means of a rapid prototyping hardware consisting on a Flexible ECU and a PXI platform. The software flashed into the ECU has been obtained by means of ETAS EHOOKS, which merges application and basic software.

Experimental tests have been carried out with a passenger car Common Rail injection system equipped with solenoid CRI 2.20 injectors of latest generation and both single and pilot-main schedules have been considered. The performance of the newly designed closed-loop control strategy has been compared with a previously developed control, in which two pressure signals were measured along the pipe feeding the injector to measure the mass at the injector inlet.

The results on single injections showed that the new control strategy is capable of reducing the error in the injected quantity below 0.6 mg for all the considered working condition. The control system is capable of compensating the drift, due to the different thermal regime experienced by the injector. If the fuel tank temperature is varied from 40 °C to 68 °C an error in the injected mass up to 2 mg can be noticed for the standard system, while the new closed-loop control features an accuracy below 1 mg, in line with the previously developed closed-loop control applying two additional pressure sensors.

Regarding the precision, the new control strategy is not capable to give any appreciable benefits since the CRI 2.20 injection apparatus features high performance in terms of repeatability, even when is equipped with the standard control.

Finally, tests on pilot-main shots have shown the capability of the presented control to dramatically reduce the overall injected mass error when the two injection events are close to be fused. The *DT* sweeps, for fixed set of p_{nom}, M_{pil} and M_{main} values, present an error in the overall injected mass which is always below 1 mg.

In summary, the innovative architecture reaches the same control performance as in the case of a previous prototype with two additional high-pressure transducers, but with significantly lower manufacturing costs.

REFERENCES

[1] Nieder, R., Benbi, D.K., Reichl, F.X., 2018. Soil-borne Particles and Their Impact on Environment and Human Health. Soil Components and Human Health. Springer, pp. 99–177.

[2] Nanthagopal K, Ashok B, Garnepudi RS, Tarun KR, Dhinesh B. Investigation on diethyl ether as an additive with Calophyllum Inophyllum biodiesel for CI engine application. Energy Convers Manage 2019;179:104–13.

[3] Dhinesh B, Annamalai M, Lalvani IJ, Annamalai K. Studies on the influence of combustion bowl modification for the operation of Cymbopogon flexuosus biofuel based diesel blends in a DI diesel engine. Appl Therm Eng 2017;112:627–37.

[4] Zhao, Weihua, Junhao Yan, Suya Gao, Timothy H. Lee and Xiang-rong Li. “The combustion and emission characteristics of a common-rail diesel engine fueled with diesel, propanol, and pentanol blends under low intake pressures.” *Fuel* (2022), vol. 307, 121692.

[5] Funayama, Y., Yoshitomi, K., Ishii, M., Nakajima, H. et al., "Influence of Combustion Chamber Shape and In-Cylinder Density on Soot Formation in Diesel Combustion," *SAE Int. J. Adv. & Curr. Prac. in Mobility* 2(1):415-425, 2020, https://doi.org/10.4271/2019-01-2271.

[6] Yan, Wei, Teng Dou, Jinbo Wang, Nanxuan Mei and Guoxiang Li. “Research on the Influence of Euro VI Diesel Engine Assembly Consistency on NOx Emissions.” *Energies* 13 (2020): 5335.

[7] Ayodhya, Archit S. and Kumar Gottekere Narayanappa. “An overview of after-treatment systems for diesel engines.” *Environmental Science and Pollution Research* 25 (2018): 35034-35047.

[8] Zhao, J., Grekhov, L. & Yue, P. Limit of Fuel Injection Rate in the Common Rail System under Ultra-High Pressures. *Int.J Automot. Technol.* **21,** 649–656 (2020). https://doi.org/10.1007/s12239-020-0062-3

[9] Payri R, Gimeno J, Martí-Aldaraví P, Viera A. Measurements of the mass allocation for multiple injection strategies using the rate of injection and momentum flux signals. *International Journal of Engine Research*. 2021;22(4):1180-1195. doi:10.1177/1468087419894854

[10] Park, W., Ra, Y., Kurtz, E., Willems, W. et al., "Use of Multiple Injection Strategies to Reduce Emission and Noise in Low Temperature Diesel Combustion," SAE Technical Paper 2015-01-0831, 2015, doi:10.4271/2015-01-0831.

[11] Venkateswarlu, Kavati and Konijeti Ramakrishna. "Effect of turbulence and multiple injection strategies on homogeneous charge compression ignition (HCCI) diesel engines – a review." *International Journal of Ambient Energy* (2019): n. pag. 858-872

[12] d'Ambrosio, S., Ferrari, A., Mancarella, A. *et al.* Effects of Rate-Shaped and Multiple Injection Strategies on Pollutant Emissions, Combustion Noise and Fuel Consumption in a Low Compression Ratio Diesel Engine. *Int.J Automot. Technol.* **21,** 197–214 (2020). https://doi-org.ezproxy.biblio.polito.it/10.1007/s12239-020-0020-0

[13] Yarsam, Pravin, Abhijit. A. Athawale and Vaibhav kapadnis. "Adopting the Features of Digital Rate Shaping (DRS) with Multiple Injections Strategy on Small 2 Cylinder Common Rail BSVI Engine to Improve FE." *SAE Int. J. Adv. & Curr. Prac. in Mobility 4(2):688-704, 2022,*

[14] Busch, Stephen and Paul C. Miles. "Parametric Study of Injection Rates With Solenoid Injectors in an Injection Quantity and Rate Measuring Device." *Journal of Engineering for Gas Turbines and Power-transactions of The Asme* 137 (2014): 101503.

[15] Ferrari A, Mittica A. Response of different injector typologies to dwell time variations and a hydraulic analysis of closely-coupled and continues rate shaping injection schedules. Appl Energy 2016;169:899–911.

[16] Busch S, Zha K, Miles PC. Investigations of closely coupled pilot and main injections as a mean to reduce combustion noise. In: 8th thiesel conference on thermo and fluid dynamic processes in direct injection engines, Valencia; 9th–12th September,2014.

[17] d'Ambrosio S, Ferrari A. Effects of pilot injection parameters on low temperature combustion diesel engines equipped with solenoid injectors featuring conventional and rate-shaped main injection. Energy Convers Manage 2016;110:457–68.

[18] Wang L, Li G, Xu C, Xi X, Wu X, Sun S. Effect of characteristic parameters on the magnetic properties of solenoid valve for high-pressure common rail diesel engine. Energy Convers Manage 2016;127:656–66.

[19] Wintrich T, Hammer J, Naber D, Raff M, Rath C, Stapelmann A, et al. Motorsysteme. In: Liebl J, Beidl C, editors. Proceedings of the Internationaler Motorenkongress 2015. Wiesbaden: Springer Vieweg; 2015. p. 165–211.

[20] Finesso, Roberto and Ezio Spessa. "A control-oriented approach to estimate the injected fuel mass on the basis of the measured in-cylinder pressure in multiple injection diesel engines." *Energy Conversion and Management* 105 (2015): 54-70.

[21] C. J. Moreno, O. Stenlaas and P. Tunestal, "Bayesian Method for Fuel Mass Estimation of Short Pilot Injections based on its Misfire Probability," *2020 American Control Conference (ACC)*, 2020, pp. 1507-1513, doi: 10.23919/ACC45564.2020.9147866.

[22] Jorques Moreno, C., Stenlåås, O., and Tunestål, P., "Cylinder Pressure Based Method for In-Cycle Pilot Misfire Detection," SAE Int. J. Advances & Curr. Prac. in Mobility 2(2):488-502, 2020, doi:10.4271/2019-24-0017.

[23] Ferrari, Alessandro, Carlo Novara, Emilio Paolucci, Oscar Vento, Massimo Violante and Tantan Zhang. "Design and rapid prototyping of a closed-loop control strategy of the injected mass for the reduction of CO2, combustion noise and pollutant emissions in diesel engines." *Applied Energy* (2018), pages 358-367, doi: 10.1016/j.apenergy.2018.09.028

[24] Ferrari, Alessandro, Carlo Novara, Emilio Paolucci, Oscar Vento, Massimo Violante and Tantan Zhang. “A new closed-loop control of the injected mass for a full exploitation of digital and continuous injection-rate shaping.” *Energy Conversion and Management* (2018): n. pag. 629-639, doi: 10.1016/j.enconman.2018.08.037

[25] Zhang, Tantan. “An estimation method of the fuel mass injected in large injections in Common-Rail diesel engines based on system identification using artificial neural network.” *Fuel* (2021): 122404, doi: 10.1016/j.fuel.2021.122404

[26] Ferrari, Alessandro, Zhiru Jin, Oscar Vento and Tantan Zhang. “An injected quantity estimation technique based on time–frequency analysis.” *Control Engineering Practice* 116 (2021): 104910.

[27] Hammer J, Raff M and Naber D, 2014. “Advanced diesel fuel injection equipment – A never ending BOSCH story”. 14th Internationales Stuttgarter Symposium, Springer Vieweg, Wiesbaden, Germany, March 18-19, 2014.

[28] Ishiduka K, Uchiyama K, Higuchi K, Yamada N, Takeuchi K, Herrmann OE, et al. “Further innovations for diesel fuel injection systems: close-loop control of fuel quantity by i-Art & ultra high injection pressure”. 19th Aachen colloquium, Aachen, 4th-6th October; 2010.

[29] Serizawa K, Ueda D, Mikami N, Tomida Y, Weber J. “Realizing robust combustion with high response Diesel injector with controlled diffusive spray nozzle and closed loop injection control”. SAE Technical Paper 2017-01-0845; 2017

[30] Beduneau JL, Bercher P, Cardon C, Meissonnier G, Uberti Bona M, Voigt P, et al. “Proceedings of the SIA Powertrain conference”. 2014.

[31] Ferrari, A., & Zhang, T. (2019). “Benchmark between Bosch and Zeuch method–based flowmeters for the measurement of the fuel injection rate”. *International Journal of Engine Research, 22*, 316 - 327.

[32] Ferrari, A., & Vento, O. (2020). “Influence of Frequency-Dependent Friction Modeling on the Simulation of Transient Flows in High-Pressure Flow Pipelines”. *Journal of Fluids Engineering-transactions of The Asme, 142*.

[33] Ferrari, A., Mittica, A., Pizzo, P., & Jin, Z. (2018). “PID Controller Modelling and Optimization in Cr Systems with Standard and Reduced Accumulators”. *International Journal of Automotive Technology, 19*, 771-781.

[34] Jin, Z., Vento, O., Zhang, T., Ferrari, A., Mittica, A., Ouyang, L., & Tan, S. (2021). “Numerical-Experimental Optimization of the Common-Feeding Injection System Concept for Application to Light-Duty Commercial Vehicles”. *Journal of Energy Resources Technology-transactions of The Asme, 143*.

[35] Ferrari, A., & Pizzo, P. (2016). “Optimization of an Algorithm for the Measurement of Unsteady Flow-Rates in High-Pressure Pipelines and Application of a Newly Designed Flowmeter to Volumetric Pump Analysis”. *Journal of Engineering for Gas Turbines and Power-transactions of The Asme, 138*, 031604-031614.